Journal of Nuclear Materials 512 (2018) 56–64

Contents lists available at ScienceDirect

Journal of Nuclear Materials

journal homepage: www.elsevier.com/locate/jnucmat

Natural alteration of ^{6}Li alumino-silicate glass

Jamie L. Weaver [a, *], Danyal Turkoglu [b]

[a] Material Measurement Laboratory, National Institute of Standards and Technology, 100 Bureau Drive, Gaithersburg, MD, 20899, USA
[b] NIST Center for Neutron Research, National Institute of Standards and Technology, 100 Bureau Drive, Gaithersburg, MD, 20899, USA

ARTICLE INFO

Article history:
Received 13 April 2018
Received in revised form
2 August 2018
Accepted 18 September 2018
Available online 21 September 2018

ABSTRACT

Understanding the chemical durability of neutron shielding materials is necessary when assessing their long-term service potential. In this study, the chemical durability of a ^{6}Li enriched neutron shielding glass that has been exposed to natural, near-operational conditions is assessed by Prompt Gamma Activation Analysis (PGAA) and Neutron Depth Profiling (NDP). These non-destructive, nuclear analysis techniques are sensitive to ^{6}Li, and PGAA is uniquely able to detect H in low quantities in solids. It was determined that the enriched alumino-silicate glass can alter within 2 months of exposure to the natural environment. This exposure resulted in an average surface alteration layer thickness of ≈22 μm. The alteration layer contained ≈47% less ^{6}Li than the bulk glass. Alternatively, a 3 years exposed sample of the glass had a surface alteration depth of ≈30 μm and ^{6}Li depletion levels in the alteration layer were between 47% and 75% less ^{6}Li than the bulk glass. When the alteration layer on the 3 years sample was removed, the H content of the glass's surface was nearly eliminated. This sample also showed variable Li concentrations throughout the alteration volume, which contrasts with near static Li concentration in the alteration volume of the 2 months sample. From these findings it was determined that the depletion in Li at the surface of the glass will not affect the glass's neutron shielding properties, but it may change the mechanical stability of the glass's surface and, due to increased H content in the alteration layer, make it an inappropriate material for the lining of certain neutron analysis instruments.

Published by Elsevier B.V.

1. Introduction

Neutron shielding materials are installed near and around nuclear reactors, radiation point sources, and neutron scattering and activation instruments to protect the health of human researchers. Reactions of particular concern are the ^{14}N(n, p)^{14}C and ^{1}H(n, γ)^{2}H, which are responsible for most of the radiation dose delivered to the human body by thermal neutrons [1]. The products from these reactions can be effectively blocked by use of specially designed neutron shielding materials that moderate epithermal and fast neutrons, absorb thermal or cold neutrons, and shield individuals from radiation produced by nuclear reactions. Today, these materials can be purchased in a variety of materials and shielding efficiencies. Many shielding materials use ^{6}Li as a neutron absorber (Eq. (1)) because ^{6}Li has a large thermal neutron capture cross section (σ_{th} ≈ 941 b), and the gamma radiation produced from the reaction is small yield (minor γ ray branch of 0.004%, ≈37 mb). In addition to its desired nuclear properties, the production cost of ^{6}Li-doped neutron shielding is relatively inexpensive, and the isotope can be purchased in the U.S. at enrichments levels greater than 95% (natural isotopic abundance of ^{6}Li is 7.5%).

$$^{6}_{3}Li + n_{th} \rightarrow \alpha + t \quad (1)$$

where n_{th} is the incoming thermal neutron, α is an alpha particle ($^{4}_{2}He$, *2727.92* keV), and t is a triton particle ($^{3}_{1}H$, *2055.55* keV).

A detailed review of ^{6}Li neutron shielding materials used in nuclear research facilities has been previously published in Ref. [2]. Of the materials discussed, ^{6}Li-doped glass was stated as a preferred shielding material because (*i*) it can be formulated to incorporate a large atom fraction of the isotope, (*ii*) it can be formed into a variety of shapes and sizes, and (*iii*) the durability of the glass can be enhanced by the moderate addition of other elements (*e.g.*, B [3] and Al [4]) into the glass structure [2]. In regards to point *iii*, only the radiation durability of ^{6}Li neutron shielding glasses has been studied in detail [2], and the chemical durability of the glasses has received less attention. However, with an increased use of ^{6}Li glass as a neutron shield in open (*i.e.*, at atmosphere) environments, a

* Corresponding author.
E-mail address: jamie.weaver@nist.gov (J.L. Weaver).

https://doi.org/10.1016/j.jnucmat.2018.09.034
0022-3115/Published by Elsevier B.V.

need has arisen to assess the chemical durability of the glass under natural conditions.

The herein presented study addresses this need by evaluating the chemical alteration of ^{6}Li alumino-silicate neutron shielding glass (NIST K2959, [2]) that had been exposed to natural, in-door conditions for ≈ 3 years. The sample was analyzed to determine whether and to what extent the glass had altered. The glass was analyzed by Neutron Depth Profiling (NDP, [5]) and Prompt Gamma Activation Analysis (PGAA, [6]). These non-destructive techniques are sensitive to ^{6}Li, and PGAA has the additional benefit of being uniquely able to detect H, which is an element difficult to quantify by other instrumental methods and an important indicator of glass alteration [7]. Results from these two analyses were supported by data collected by Scanning electron microscopy (SEM) and X-ray Diffraction (XRD).

2. Materials and methods

The ^{6}Li glass was obtained from a batch of glass produced for PGAA collimators and as a liner for a PGAA sample chamber. This glass was intended to be a hydrogen-free material for absorbing neutrons as low-level H measurements by PGAA are a critical application [8]. Increase in the hydrogen content of the glass could result in increased hydrogen background signal during a PGAA measurement of H-containing samples. It was suspected that the glass was altered because the glass's surfaces were very cloudy in appearance. This was contrary to the mostly clear and transparent appearance of the surface when it was first cast. Altered glasses may appear cloudy at their surfaces because the alteration layer(s) on the surface of the glass will have pores or solid masses (crystallites) that can scatter incoming light. Glass transparency can also be affected by how a glass surface is machined. The glass sample analyzed and presented in this study had not been exposed to radiation prior to these analyses, nor extensively handled after being cast, and was stored at atmosphere since its production in the fall of 2014.

The 3 years exposed ^{6}Li glass was tested for alteration by (*i*) NDP, to measure the relative concentration ^{6}Li at and near the glass surface, (*ii*) PGAA, to measure the amount of H and other glass forming elements, (*iii*) SEM, to visually inspect cross-sections of the exposed glass, and (*iv*) XRD, to test for devitrification of the glass. One side of a sample of the exposed glass had (36.8 ± 1.0) μm of the surface removed by dry sanding with variably-decreasing grits of Silicon Carbide grinding papers (MicroCut, Buehler). The amount of material removed was measured in triplicate at three points along the glass's surface with a digital micrometer (293 MDC-MX Lite, Mitutoyo). This sanding was necessary as the first NDP results (Fig. 1a–b and detailed below) showed that the alteration layer extended beyond the measurement ability of the NDP for this material (>20 μm from the glass surface). Removing part of the alteration layer allowed for a deeper measurement into the glass. Dry sonication in an inverted position, followed by a cleaning with compressed and oil-filtered nitrogen gas, were used to remove sanding debris. This cleaning process was repeated twice to ensure a clean surface. SEM of the sanded glass's surface showed no signs of fines or other particulates. No liquid lubricants were used in the surface preparation process as there was a concern that the chemicals may remove Li or part of the alteration layer from the glass. The 3 years exposed, and sanded glass sample was approximately 30 mm × 35 mm × 10 mm.

A section of a glass sample was cross-sectioned to expose a fresh, unexposed glass surface. The cut was completed with an ethanol cleaned diamond tipped blade using an IsoMet, Low Speed Saw (Buehler). A small amount of powdered graphene was used to lubricate the saw during cutting to reduce heat buildup and sample damage. A soft brush was used to remove most of the graphene from the cut surface before SEM was conducted. As compared to the exposed surface and the sanded surface, the broken surface should have relatively little physiosorbed water [9], and should not have water penetrating the glass surface. The exposed, sanded, and freshly-broken surfaces were analyzed by NDP to determine the extent of alteration of the glass. In a subsequent study, the sanded glass surface was exposed to atmosphere for ≈2 months in the same open environment in which the glass was originally stored. At the end of the 2 months, the sanded glass surface was remeasured by NDP to determine if the freshly-sanded surface had become depleted in ^{6}Li.

3. Experimental

3.1. NDP

NDP and PGAA experiments were completed at the National Institute of Standards and Technology (NIST) Center for Neutron Research (NCNR). The 20 MW research reactor in the NCNR contains a liquid hydrogen cold source at ≈ 20 K, which provides cold neutrons. NDP spectra were acquired at the Neutron Guide 5, Cold Neutron Depth Profiling station. A circular aperture made of 0.5 mm thick Teflon (fluorinated ethylene propylene (FEP)) with a 10.0 mm diameter opening was mounted to an Al disk with a large (>30 mm) hole in its center. The NDP results presented here are the average ^{6}Li distributions across the surface area of Teflon aperture opening.

Each glass sample was irradiated at a near constant fluence rate of cold neutrons; any variations were corrected via a neutron monitor during data processing. All experiments were conducted under vacuum and near room temperature. NDP spectra were collected for ≈4 h per spot. Both ^{6}Li nuclear reaction products, α and *t* particles, were detected using a circular transmission-type silicon surface-barrier detector that was positioned ≈120 mm from the sample surface. Each spectrum was corrected for dead time (≈1.4%) and background noise. The α profiles were corrected for interference by the *t* profiles by using linear regression analysis (SigmaPlot, 14.0) to fit the linear portion of the *t* profile, and then subtracting the calculated fit from the corresponding α profile. While this method will not allow for quantitative assessment of the α profiles, it will enable qualitative comparison between the α profiles of different samples. A detailed description of the NDP setup and data processing steps can be found in Ref. [10]; however, the neutron guide at which the instrument was located has changed since the publication of the cited article.

The *t* and α particle interactions with the lithiated, alumino-silicate glass were modeled in SRIM (2008, [11]), assuming a pristine glass density of 2.42 g/cm^{3} (as reported in Ref. [2]) an altered glass density of 1.50 g/cm^{3} (value based on reported literature values for density of alkali-alumino-silicate glass alteration layer densities [12,13]), and starting *t* and α particle energies of 2727.92 keV and 2055.55 keV, respectively. ^{6}Li concentrations were calculated from the known concentration of ^{10}B in a B-implanted concentration standard (in-house), according to Eq. (2):

$$[a] = [b]\frac{\sigma_{0,b}}{\sigma_{0,a}} \tag{2}$$

where *[a]* and *[b]* are the concentrations (atoms/cm^{2}) of isotopes *a* and *b* being measured in the sample and standard, respectively, and σ_0 is the thermal neutron cross-section for the charged-particle emission.

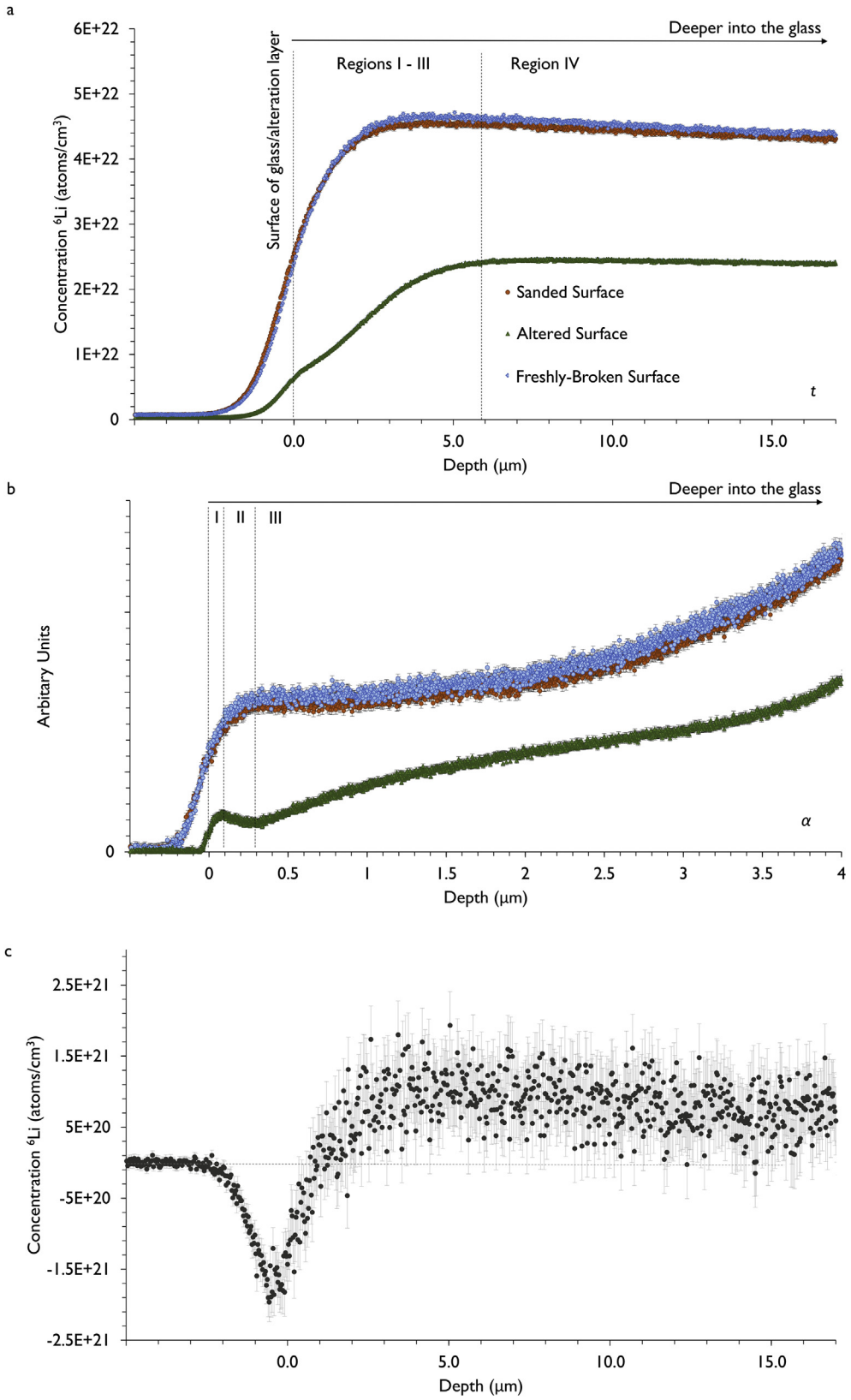

Fig. 1. a. NDP *t* particle profile of ^{6}Li concentration versus depth of the 3 years exposed glass (green), sanded glass (brown), and freshly broken glass (blue) surfaces. The exposed glass showed depletion of ^{6}Li at its surface, indicating glass alteration. b. NDP α particle profile of ^{6}Li concentration vs. depth of the exposed glass (green), sanded glass (brown), and fresh broken glass (blue) surfaces. Results support *t* depth profile and SEM analysis of exposed glass surface (see Fig. 2). c. Subtracted *t* profile of freshly-broken glass and sanded glass. Beyond $\approx$1 μm depth the ^{6}Li concentration becomes generally positive, indicating that the surface of the sanded glass contained slight less Li than the freshly-broken glass surface. Dashed gray line is at 0. Error bars are the calculated fractional errors of measurement and were calculated from experimental counting statistics. (For interpretation of the references to colour in this figure legend, the reader is referred to the Web version of this article.)

3.2. PGAA

Isotopic analyses of the 3 years exposed and sanded ^{6}Li glasses were performed at the cold neutron PGAA instrument located at Neutron Guide D in the NCNR. The ^{6}Li glass was placed in a Teflon FEP bag, which was heat sealed shut, and then suspended from aluminum wires spanning the sample holder frame. The sanded and exposed portions of glass were measured separately to determine changes in nominal elemental concentrations between the two surfaces. The samples were each measured for 3.0 h and 18.0 h, respectively, both with 1.4% detector dead time. As a blank, a Teflon FEP bag was measured to obtain a background spectrum for 3.9 h with 0.3% dead time. Background peak counts rates were subtracted from the corresponding peak count rates in experimental data. Full-energy detection efficiency (ε) was calibrated from 50 keV to 11 MeV with measurements of decay gamma rays from ^{133}Ba and ^{152}Eu sources and prompt gamma rays emitted by N, Cl and Ti in urea, NaCl and Ti foil samples, respectively. Peak fitting and detection efficiency calibration were performed with Hypermet PC [14].

The atom ratios of element x to element y were determined using the relative approach shown in Eq. (3), where ρ_{γ} is the peak count rate, $\varepsilon(E_{\gamma})$ is the full energy detection efficiency and σ_{γ} is the partial gamma-ray production cross section [9]. The elemental cross section values were taken from the Evaluated Gamma-ray Activation File (EGAF) for H, Al, and Si [15]. Updated isotopic cross sections for ^{6}Li and ^{7}Li from Ref. [16] were used to determine the enrichment of ^{6}Li to be (96 ± 1) atom %. Atom ratios of Li/Si and Al/Si were determined using Eq. (3):

$$\frac{n_x}{n_y} = \frac{(\rho_{\gamma_1,x} - \rho_{\gamma_1,blank}) \Big/ \varepsilon(E_{\gamma_1})}{(\rho_{\gamma_2,y} - \rho_{\gamma_2,blank}) \Big/ \varepsilon(E_{\gamma_2})} \frac{\sigma_{\gamma_2,y}}{\sigma_{\gamma_1,x}} \quad (3)$$

The atom fractions, expressed as oxides, of Al, Si, and Li in the glass, were determined. Table 1 compares the measured glass composition to the nominal composition of the glass as published by Stone et al. [2].

3.3. XRD and SEM

X-Ray diffraction (XRD) was conducted at the NIST's Center for Nanoscale Science and Technology (CNST) with a Rigaku SmartLab X-Ray Diffraction. XRD data was collected and plotted using SmartLab (Rigaku). High contrast SEM images were taken using a Zeiss Ultra 60 Field Emission Scanning Electron Microscope housed within CNST with an in-lens secondary detector. The samples were mounted on edge with carbon tape. All images were taken at a ≈5.0 mm working distance, 5.0 kV, and with a 30.0 mm aperture. SEM image processing and alteration layer thickness measurements were completed in ImageJ (ver. 1.48k, 2013 [17]). A summary of alteration layer thicknesses is presented in the SI (Tables 1 and 2).

Table 1
Comparison of the measured glass compositions of the 3 years exposed and sanded sides of the ^{6}Li glass to the nominal formula as determined by PGAA.

Compound	Atom fraction (%)		
	Nominal [2]	3 Years Exposed	Sanded
Li_2O	37	37.1 ± 0.8	37.2 ± 0.8
SiO_2	59	58.9 ± 0.8	58.8 ± 0.8
Al_2O_3	4	3.9 ± 0.1	4.0 ± 0.1

Gamma ray energies in keV for peaks used for analysis:
^{6}Li: 6769.5, 7246.7.
^{7}Li: 2032.3.
Si: 1273.3, 2092.9, 3539.0, 4933.9, 7199.2.
Al: 1778.9, 3465.1, 4133.4, 4259.5, 4733.8.

Table 2
Data and PGAA results used to determine the experimental R_{Si}/R_H values.

Element	E_{γ} (keV)	σ_{γ} (b)	Peak count rate[a] (s^{-1})	R_{Si}/R_H
H	2223.25	0.3326 ± 0.0007	0.456 ± 0.007	n/a
Si	2092.90	0.0331 ± 0.0006	2.00 ± 0.03	22.8 ± 0.5
Si	3538.97	0.1190 ± 0.0020	7.42 ± 0.10	23.5 ± 0.5
Si	4933.89	0.1120 ± 0.0023	6.92 ± 0.10	23.3 ± 0.6

[a] Corrected for background and efficiency.

4. Results

4.1. Comparison of 3 years exposed, sanded, and freshly broken glass profiles

4.1.1. NDP

NDP results of the 3 years exposed, sanded, and freshly broken surfaces are shown in Fig. 1. The profile of the exposed glass shows depletion of ^{6}Li at the near-surface, which is an indication of glass alteration. The probing depth for the t energy spectrum (≈21 μm), was less than the SEM estimated alteration layer thickness ((37.4 ± 8.2) μm, Fig. 2a). To measure deeper into the glass surface, ≈30 μm of surface material was sanded off the exposed glass, the surface was cleaned, and the sample was remeasured by NDP. These results were compared to the NDP profile of the freshly-broken glass surface to determine if the sanding removed the alteration layer. The ^{6}Li t profile of the sanded glass generally showed a slightly lower concentration of ^{6}Li across the alteration layer than that of the freshly-broken glass sample (Fig. 1c). This result suggests that the entire alteration layer was not removed by sanding. The estimated NDP ^{6}Li depletion layer thickness, which is assumed to be approximately equal to the depth to which alteration penetrated the glass, is > 30 μm. This finding is in accordance with the SEM results (Fig. 2a), which suggest an average alteration layer thickness of (37.4 ± 8.2) μm (see SI).

The t profile of the exposed glass shows that ^{6}Li is not uniformly distributed in the depleted regions of the glass. This finding is supported and shown in greater detail by the α particle NDP data presented in Fig. 1 b. The α particle has a lower recoil energy and is a heavier mass than the t, and, therefore, will be stopped within the material at a much faster rate than the t particle. The α profile shows that there are three (3) distinct regions of variable Li concentration. A fourth region can be identified in the t profile. Different concentrations of Li in these regions could be indications of variability in the alteration layer structure at these sites, a theory which is discussed further in the *Discussion* section. The depletion of Li in these regions relative to that measured in the freshly broken glass sample ranges from ≈75% (measured from region I) to ≈ 47% (measured in region IV).

4.1.2. PGAA

Assuming a homogenous sample in determining atom ratios of $1/v$ absorbers with PGAA obviates the need for characterizing the neutron beam's intensity and spectrum because the neutron fluence rate cancels out in the ratio. However, the ^{6}Li glass is assumed to be inhomogeneous with its composition and density varying in the alteration layer due to Li migration and the uptake of moisture from the air, while the bulk glass likely remains nominal. This assumption was proved true by the NDP results (see NDP results in next section). Therefore, modeling of the neutron beam's intensity as a function of the glass's variable chemistries is needed to calculate correct atom fractions. Furthermore, the neutron self-shielding by the glass biases the results towards measuring the

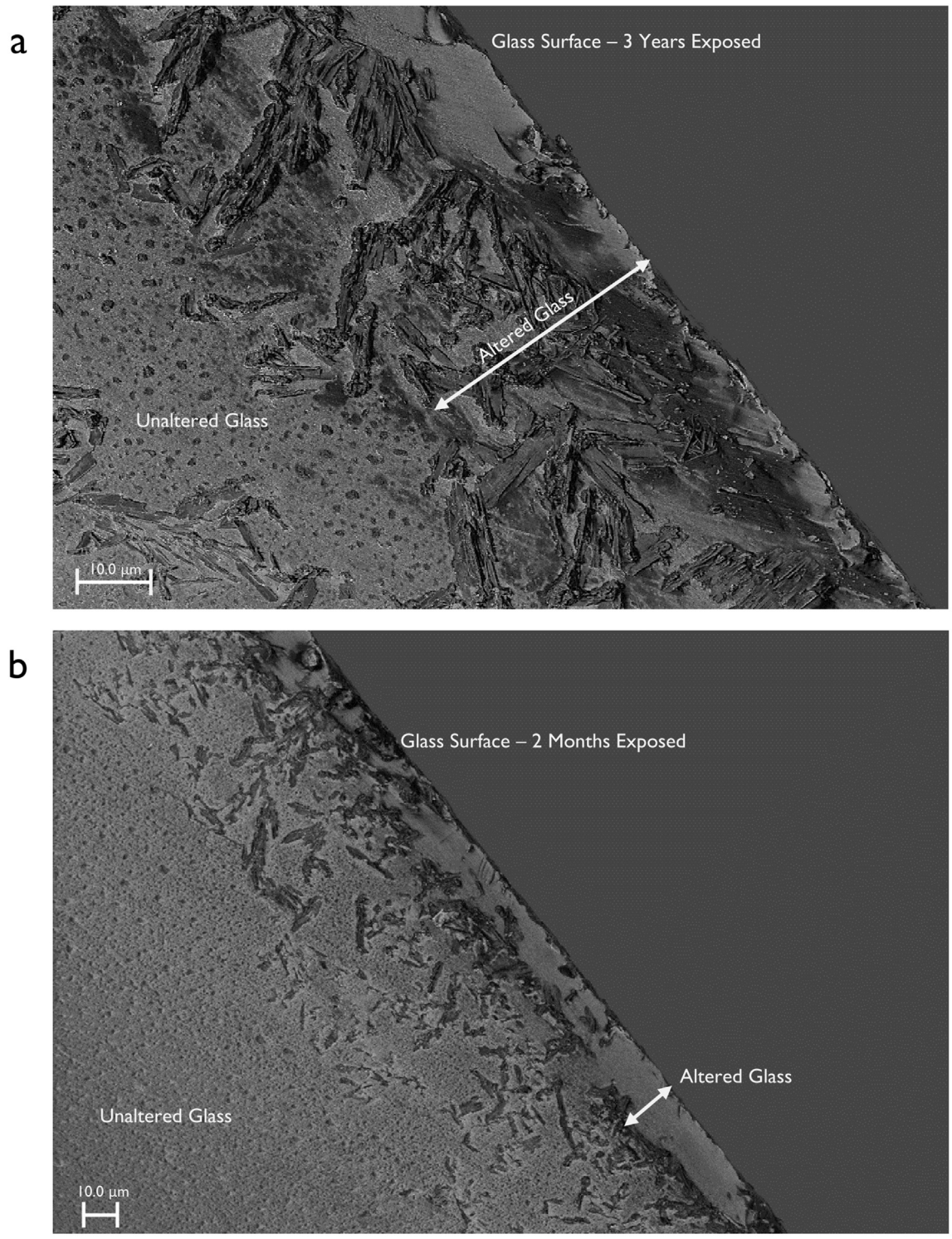

Fig. 2. a. In-lens SEM image of alteration layer formed on surface of 3 years exposed neutron shielding glass. The alteration layer appears to be approximately 30 μm thick, which agrees with NDP results. Lathe-like structures on the cut surface are graphene and are artifacts from sample cutting. b. In-lens SEM image of alteration layer formed on surface of ≈2 months exposed neutron shielding glass. Alteration layer appears to be > 20 μm thick, which agrees with NDP results.

surface that is irradiated by the peak neutron fluence rate. These issues are addressed below through the development of a way to estimate the H contained within the alteration layer from experimental and modeling results.

Models of the alteration layer for the 3 years exposed ^{6}Li glass samples were developed based on NDP and SEM results. The following assumptions were made in the development of the models: (*i*) The alteration layer is ≈ 37 μm thick and is a homogeneous composition, (*ii*) the density of the alteration layer is 1.5 g/cm^3, reduced from the nominal 2.42 g/cm^3 density, and (*iii*) the NDP results showed that the ^{6}Li atom density was depleted by 75% near the surface and by 47% near the end of the alteration layer.

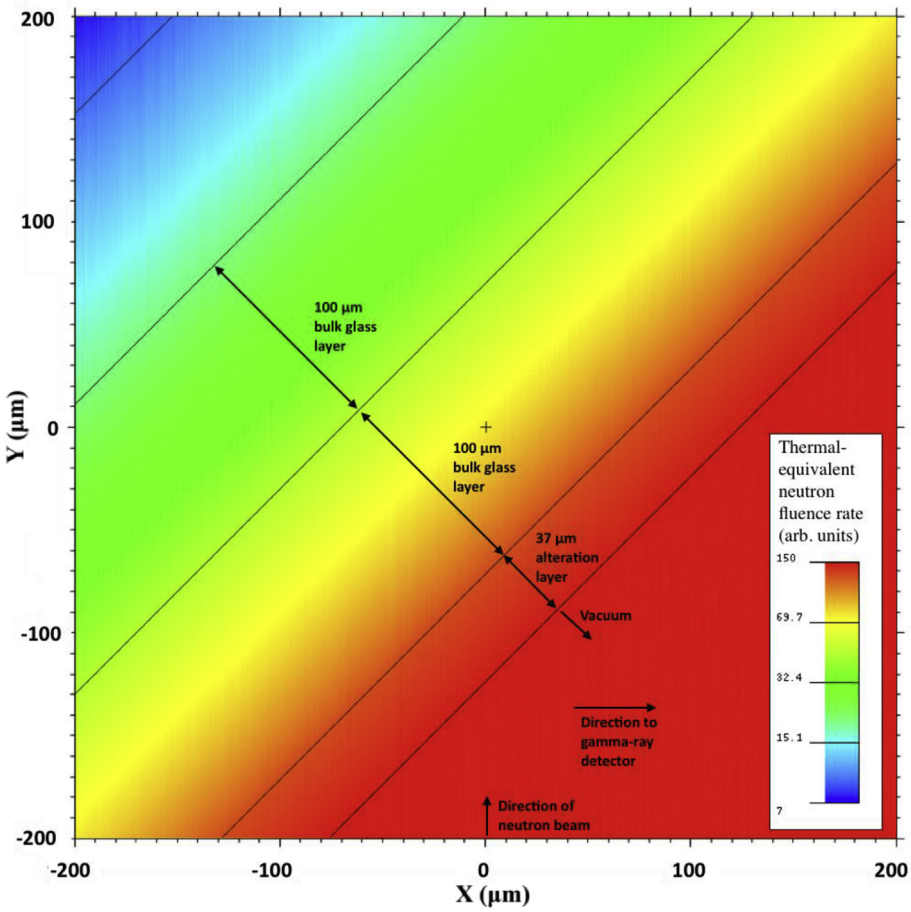

Fig. 3. MCNP6 mesh tally of the thermal-equivalent neutron fluence rate for the ^{6}Li glass model of Case 2b in the PGAA neutron beam. Note the sample is situated at a 45° angle to the detector and neutron beam.

Based on these results and the assumption of a reduced density of 1.5 g/cm^3, three cases were tested with the ^{6}Li atom density reduced to 47% (Case 1), 39% (Case 2) and 25% (Case 3) of the nominal value, while the amount of H in the alteration layer was proportional to the amount of Li depleted. Two subcases were tested: (Subcase a) 0.01 H atom added per Li atom lost and (Subcase b) 0.1 H atom added per Li atom lost, and the amount of Si, Al and O comprised the remainder of the composition in the same proportions as the bulk glass.

A detailed MCNP6 [18] model of the PGAA instrument, including estimates for the neutron intensity and spectrum from neutron guide simulations, was used to find the neutron capture reaction rates for H (R_H) in the alteration layer and for Si in the alteration layer and bulk glass (R_{Si}). The ratio (R_H/R_{Si}) measured by PGAA rates are shown in Table 2 in addition to the gamma-ray energies, cross sections, and experimental peak count rates. The reported reaction rates were corrected for gamma-ray emission probabilities. In the MCNP6 model, the alteration layer and the bulk glass were split into 1 μm thick and 100 μm thick layers, respectively. Fig. 3 shows a mesh tally of the relative thermal-equivalent neutron fluence rate for the Case 2b model with 61% Li depletion and with 0.1 H atoms added per Li atom lost. Additionally, the relative reaction rates for neutron capture for ^{1}H and Si in each layer were found by fluence rate tallies (F4) weighted by the energy-dependent neutron capture cross sections of ^{1}H and Si, respectively. Fig. 4a and Fig. 4b show the relative neutron fluence rate values in the alteration and bulk layers, respectively, for the model with 61% Li depletion and with 0.1 H atoms added per Li atom lost.

The compositions of the alteration layer for each subcase are shown in Table 3. The subcases of Case 1 (0.01 H atoms added per Li atom lost) and Case 2 (0.1 H atoms added per Li atom lost) produced reaction rate ratios that bracketed the experimental results ($\approx$ 23). Using the H mass fraction of 1.5 mg/g for the Case 2b model with 61 % Li depletion and 0.1 H atoms per Li atom lost, the areal mass density of H in the alteration layer is 8.33 μg/cm^2. A water layer (at STP) with a similar areal mass density has a thickness of 0.75 μm.

The background-corrected H count rates for the exposed and sanded sides were (1.381 ± 0.014) s^{-1} and (0.186 ± 0.005) s^{-1}, respectively. The background was subtracted by using the peak ratio of H to F (from the Teflon) measured in the blank. As shown in Fig. 4, the thermal-equivalent neutron fluence rate decreases by approximately an order of magnitude within 200 μm depth of the surface. Thus, the PGAA measurements of the ^{6}Li glass were weighted toward measuring the surface and near-surface composition of the samples (i.e., <0.5 mm depth).

PGAA results for the exposed and sanded glasses are summarized in Tables 1 and 2. These measurements indicate a conservation of elemental concentrations between the two samples except for H. H content was higher in the exposed sample than it was in the sanded sample, suggesting that H was removed with sanding. The approximate mass fraction of H in the alteration layer of the 3 years exposed glass was estimated with the previously-discussed MCNP6 model to be between 0.12 mg/g and 1.9 mg/g. That is, between 0.01 and 0.1 H atoms were added per each ^{6}Li lost from the alteration layer. The discrepancy in amount of Li depletion depicted in the NDP data and the lack thereof in the PGAA data are most

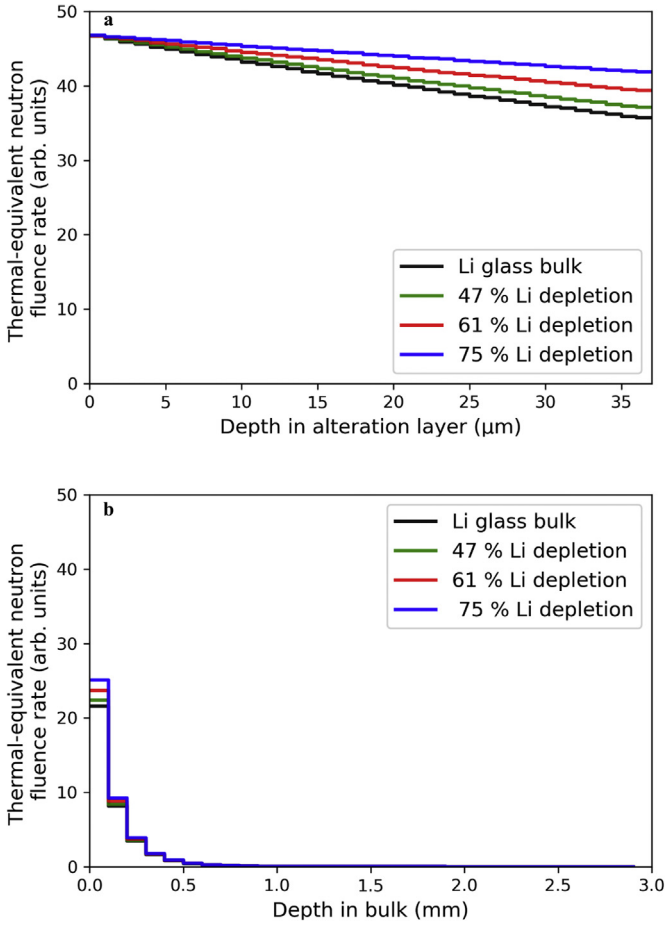

Fig. 4. Thermal-equivalent neutron fluence rate values for the 61% Li depletion case with 0.1 H atoms added per Li atom lost (a) in the first 37 μm (the alteration layer) and (b) the bulk sample up to 3 mm depth.

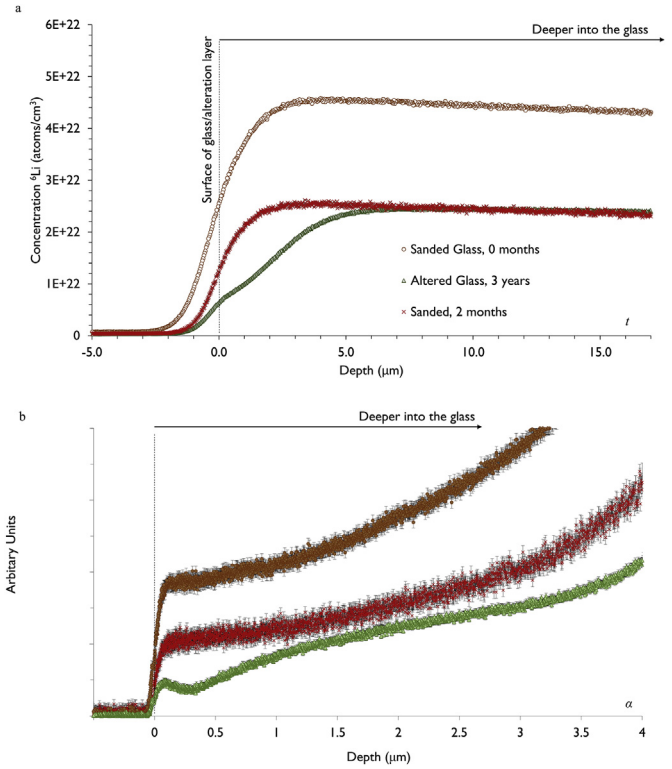

Fig. 5. a. NDP *t* particle profile of ^{6}Li concentration verses depth of sanded glass at 0 months (aka *sanded glass*, brown), 2 months (red) after sanding, and 3 years exposed glass (green). b. NDP α particle profile of ^{6}Li concentration verses depth of sanded glass at 0 months (brown), 2 months (red) after sanding, and 3 years exposed glass (green). Error bars are the calculated fractional errors of measurement and calculated from experimental counting statistics. (For interpretation of the references to colour in this figure legend, the reader is referred to the Web version of this article.)

likely because PGAA is significantly less sensitive to Li than NDP and is, in this case, a bulk measurement of the near surface up to ≈0.5 mm depth.

4.1.3. XRD

No minerals were observed by SEM on the surface of the exposed glass. The presence of a mineral (often a clay or zeolite) at or near a glass surface can be another indicator of alteration [19]. XRD of the 3 years exposed glass surface only indicated the presence of an amorphous material (see SI, Fig. 1).

4.2. Months alteration study

To determine the approximate rate of alteration, the sanded glass sample was exposed to atmosphere at the NCNR for ≈2 months between May 8, 2017 and July 13, 2017. The NCNR cold-

Table 3
Compositions, fluence rate and reaction rate ratios for each subcase in the MCNP6 modeling.

	Bulk glass	Case 1a	Case 1b	Case 2a	Case 2b	Case 3a	Case 3b
Li depletion in alt. layer	*n/a*	47%	47%	61%	61%	75%	75%
H atoms per Li atoms lost	*n/a*	0.01	0.1	0.01	0.1	0.01	0.1
Element	Mass fraction						
^{6}Li	0.0944	0.0807	0.0807	0.0594	0.0594	0.0381	0.0381
O	0.5360	0.5441	0.5434	0.5567	0.5538	0.5693	0.5682
Al	0.0423	0.0430	0.0429	0.0440	0.0429	0.0450	0.0449
Si	0.3272	0.3321	0.3317	0.3398	0.3393	0.3475	0.3469
H		0.00012	0.0012	0.00015	0.0016	0.00019	0.0019
Relative reaction rate							
R_H (Alt. layer)	*n/a*	1.0	9.1	1.3	11.9	1.7	14.6
R_{Si} (Alt. layer)	n/a	7.9	7.3	8.3	7.4	8.7	7.6
R_{Si} (Total)	38.5	39.7	39.0	41.7	40.8	43.8	42.7
R_{Si}/R_H							
Total	*n/a*	40.5	4.0	31.9	3.1	26.5	2.6

neutron guide hall is temperature controlled at ≈ 21.1 °C, although it has been measured to fluctuate throughout the day by a few degrees C as a function of outside weather conditions. Similarly, the guide hall's relative humidity is ≈ 50% and has been noted to fluctuate within a 24h period by > 5%. This value also changes based on outside weather conditions, as well as the number of people working in the guide hall. According to the National Weather Service record, the average maximum/minimum for May, June, and July in the Baltimore/Washington D.C. area were 23.3 °C/13.9 °C, 30.2 °C/20.1 °C, and 32.2 °C/23.0 °C, respectively [13]. The average relative humidity was 69%, 62%, and 68%. Alteration of the glass's surface was expected to occur given these warm and humid conditions.

A comparison of the NDP results for the freshly sanded (0 month), 3 years exposed, and 2 months exposed samples are presented in Fig. 5a-b. Both the *t* and *α* particle profiles show a depletion in Li in the 2 months exposed surface as compared to the 0 month exposed surface. ^{6}Li depletion levels are generally similar between the 2 months exposed and 3 years exposed samples. However, the profiles of the 3 years exposed glass show that the ^{6}Li concentration in the alteration layer varies as a function of depth. This is different from the 2 months altered glass which shows uniform depletion across the surface of the alteration layer. The alteration depth of the 2 months exposed sample (determined from the *t* profile shown in Fig. 3a) extends beyond the measurement depth of the NDP. The approximate thickness of the alteration layer as determined by SEM was (22.4 ± 4.0) μm (see Fig. 5b and SI Table 2). The range and standard deviation in alteration layer thicknesses for the 2 months exposed sample was significantly smaller than that for the 3 years exposed sample: ± 4.0 μm vs. ± 8.2 μm. No PGAA measurement of the 2 months exposed glass was conducted due to an instrument outage.

5. Discussion

It is apparent from the NDP and SEM results that the 3 years and 2 months exposed ^{6}Li neutron shielding glass samples have undergone alteration. Additionally, the approximate extent of the Li depletion from the two glasses is similar, with a minimum ^{6}Li surface depletion of about 47% for both samples. These findings suggest that alumino-silicate ^{6}Li neutron shielding glass can undergo significant, measurable alteration relatively quickly (within 2 months) when exposed to a naturally warm and humid environment.

The 3 years exposed glass was measured by PGAA to have a significant increase in H relative to the sanded glass. Also, the NDP data indicates that the ^{6}Li distribution throughout the alteration layer varies as a function of depth. From Fig. 1(a and b) it is apparent that the Li concentration is higher in region I vs. region II, and higher in region II vs. region III. These two results suggest that the alteration layer will not shield neutrons to the same extent as would be expected for the original glass and that the shielding power may vary across the alteration depth. The depletion in ^{6}Li will result in less neutrons being absorbed within the first 10's of μm of the glass surface, and the increased in H will cause more neutrons to scatter. Additionally, the mechanical durability of the hydrated alteration layer is most likely less than that of the glass. This layer may be more prone to delaminating and fracturing, which may not only decrease the overall shielding ability of the glass, but, also, cause the release of material embedded with radioactive tritium. This previous scenario has not, to the extent of our research, been reported to occur for this glass. Also, the alteration layer thickness is orders of magnitudes smaller than that of the glass: ≈ 37 μm vs. 1E+7 μm, respectively. Therefore, the loss of the alteration layer will most likely not significantly influence the overall neutron shielding power of the glass.

The changes in ^{6}Li concentration across the alteration surface indicates possible changes in structure, and therefore density, of the altered regions. This phenomenon has been reported before for alumino-silicate glasses that have been altered for more than 100 days [20,21]. This finding brings to question the accuracy of the depth scale displayed in Figs. 1 and 5. A single density, 1.50 g/cm^{3}, was used in the NDP energy-to-depth calculation for the depth scale of the altered glass samples. The use of this value is logical because it corresponds to densities reported for alteration layers found on similar types of glasses [9,10], and the calculated profile agrees with the alteration thicknesses measured from the SEM images collected on the same sample. If the density used to calculate the depth scale for the NDP data were grossly incorrect, then the SEM thicknesses would not have matched the NDP results. However, the 1.5 g/cm^{3} density is most likely close to the average density of the alteration region and does not account for the variety of densities that may be present. One analysis method that may allow for measurement of the variable densities within the alteration region is x-ray reflectivity. X-ray reflectivity tests were executed on the 3 years and 2 months exposed samples, but the experiments did not yield meaningful results due to the surface of the samples being too rough.

The alteration of the glass may have the most significant effect on its use as a low H background shielding material for a PGAA instrument [8]. As the glass alters, more H may become incorporated in the exposed glass surface, thus increasing background H counts. This could complicate the measurement of materials containing low-level H by PGAA, particularly if the H incorporation is not constant. Therefore, it may be necessary to keep the glass-lined section of the instrument under vacuum to avoid additional alteration to the glass. Other applications for the glass, such as apertures or transmission applications, may not be significantly affected by the presence of a hydrated alteration layer.

6. Conclusion

Analysis by NDP and PGAA of a ^{6}Li glass used as neutron shielding was completed to determine if and to what extent the glass had altered. PGAA results showed an increase in H content in the 3 years exposed sample relative to the sanded sample, although native glass forming element concentrations were determined to be the same (within error). NDP measurements indicated a minimum depletion of 47% and maximum depletion of 75% in ^{6}Li in the 3 years exposed glass surface, and SEM suggested an alteration depth ≈37 μm. A similar depletion amount was found for a 2 months exposed sample of the glass, with an estimated alteration depth of ≈22 μm. These results suggest that ^{6}Li enriched neutron shielding glass can alter relatively quickly. However, the amount of ^{6}Li released by alteration relative to that contained in the unaltered glass bulk is relatively small, and the overall neutron shielding properties of the glass should not be significantly diminished.

7. Data availability

The raw/processed data required to reproduce these findings cannot be shared at this time as the data also forms part of an ongoing study.

Acknowledgments

The authors would like to thank Dr. Greg Downing, Dr. Heather Chen-Mayer, Dr. Kerry Siebein, Dr. Jeremy Cook, and Dr. Pam Chu for their mentorships and support in implementing this study. Additional thanks to the NIST Center for Neutron Research (NCNR)

and Center for Nanoscale Science and Technology (CNST) at NIST for their technical support. Partial funding for this research was provided by the United States National Research Council. Trade names and commercial products are identified in this paper to specify the experimental procedures in adequate detail. This identification does not imply recommendation or endorsement by the authors or by the National Institute of Standards and Technology, nor does it imply that the products identified are necessarily the best available for the purpose. Contributions of the National Institute of Standards and Technology are not subject to copyright.

Appendix A. Supplementary data

Supplementary data to this article can be found online at https://doi.org/10.1016/j.jnucmat.2018.09.034.

References

[1] N.R. Council, Health Effects of Exposure to Low Levels of Ionizing Radiation: BEIR V, vol. 5, National Academies, 1990.
[2] C. Stone, et al., 6Li-doped silicate glass for thermal neutron shielding, Nucl. Instrum. Methods Phys. Res. Sect. A Accel. Spectrom. Detect. Assoc. Equip. 349 (2–3) (1994) 515–520.
[3] B.C. Bunker, et al., The effect of molecular structure on borosilicate glass leaching, J. Non-Cryst. Solids 87 (1) (1986) 226–253.
[4] L.L. Hench, D.E. Clark, Physical chemistry of glass surfaces, J. Non-Cryst. Solids 28 (1) (1978) 83–105.
[5] R. Downing, et al., Neutron depth profiling: overview and description of NIST facilities, J. Res. Natl. Inst. Stand. Technol. 98 (1) (1993) 109.
[6] R.M. Lindstrom, Z. Révay, Prompt gamma neutron activation analysis (PGAA): recent developments and applications, J. Radioanal. Nucl. Chem. 314 (2) (2017) 843–858.
[7] L. Hench, Characterization of glass corrosion and durability, J. Non-Cryst. Solids 19 (1975) 27–39.
[8] D. Turkoglu, et al., Assessment of PGAA capability for low-level measurements of H in Ti alloy, Analyst 142 (2017) 3822–3829.
[9] E.A. Leed, C.G. Pantano, Computer modeling of water adsorption on silica and silicate glass fracture surfaces, J. Non-Cryst. Solids 325 (1) (2003) 48–60.
[10] R.G. Downing, Enhanced reaction rates in NDP analysis with neutron scattering, Rev. Sci. Instrum. 85 (4) (2014) 045109.
[11] J. Ziegler, SRIM & TRIM, 2008.
[12] J.T. Reiser, et al., The use of positrons to survey alteration layers on synthetic nuclear waste glasses, J. Nucl. Mater. 490 (2017) 75–84.
[13] C.L. Trivelpiece, et al., Glass surface layer density by neutron depth profiling, Int. J. Appl. Glass Sci. 3 (2) (2012) 137–143.
[14] B. Fazekas, et al., Introducing HYPERMET-PC for automatic analysis of complex gamma-ray spectra, J. Radioanal. Nucl. Chem. 215 (2) (1997) 271–277.
[15] R. Firestone, et al., EGAF: measurement and analysis of gamma-ray cross sections, Nucl. Data Sheets 119 (2014) 79–87.
[16] R. Firestone, Z. Revay, Thermal neutron radiative cross sections for Li 6, 7, Be 9, B 10, 11, C 12, 13, and N 14, 15, Phys. Rev. C 93 (5) (2016) 054306.
[17] W. Rasband, ImageJ Software, National Institutes of Health, Bethesda, MD, USA, 1997, 2012.
[18] MCNP 6.1.1, Los Alamos National Laboratory, 2017.
[19] E.C. Buck, J.K. Bates, Microanalysis of colloids and suspended particles from nuclear waste glass alteration, Appl. Geochem. 14 (5) (1999) 635–653.
[20] D. Rebiscoul, et al., X-ray reflectometry characterization of SON 68 glass alteration films, J. Non-Cryst. Solids 325 (1) (2003) 113–123.
[21] D. Rebiscoul, et al., Morphological evolution of alteration layers formed during nuclear glass alteration: new evidence of a gel as a diffusive barrier, J. Nucl. Mater. 326 (1) (2004) 9–18.